

Quasi-phase matched nonlinear media: Progress towards nonlinear optical engineering

Valdas Pasiskevicius*, Gustav Strömqvist, Fredrik Laurell, Carlota Canalias

Department of Applied Physics, Royal Institute of Technology, KTH, Roslagstullsbacken 21, 10691 Stockholm, Sweden

ARTICLE INFO

Article history:

Received 15 November 2010
Received in revised form 8 July 2011
Accepted 22 July 2011
Available online 3 September 2011

Keywords:

Nonlinear optical materials
Quasi-phase matching

ABSTRACT

Nonlinear optics has been enabled by the invention of the laser 50 years ago, and since then both technologies evolved together complementing and enabling each other. In this paper we attempt to briefly overview the historic development of second-order nonlinear materials and try to discern the trends which might dominate developments in the future. The advent of methods of quasi-phase matching and added degrees of freedom in managing three-wave mixing processes pushed the field of nonlinear optics into the realm of engineering. This trend, we believe will continue in the future. In this text we give a short description of design principles of one-dimensional and two-dimensional quasi-phase matched structures and emphasize the increased functionality afforded by such structures. We also overview the nonlinear media where engineering of nonlinear interactions has been demonstrated with the primary focus on ferroelectric and semiconductor nonlinear crystals.

© 2011 Elsevier B.V. All rights reserved.

1. Introduction historical remarks

Year 2010 marks half of a century since the first laser action demonstration in ruby by Maiman [1]. The research effort in lasers was already substantial at that time and the ruby laser was followed by demonstrations of lasing in other solid-state dielectric hosts in a rapid succession [2–4]. Laser emission from GaAs p–n junctions have been also demonstrated in 1962 [5], although the technology had to be improved by introduction of double heterostructures before it became the major contender in the laser applications field. The significance and usefulness of the technology has been perceived early on, even before the invention of the ruby laser. The fact that large part of the early laser technology development was done in well-funded industrial labs [2–5] and the remarkable speed at which the newly appearing lasers were commercialized attests to the great expectation that the laser would be one of those technologies which can revolutionize broad range of existing applications and open up new ones. The brief span of history since the laser invention indeed bears witness that these expectations were indeed met and exceeded. The subsequent laser technology development brought about laser sources at wavelength ranges from ultraviolet to sub-millimeter as well as unprecedentedly high peak powers and excellent spatial and temporal coherence properties.

High peak power of coherent radiation immediately opens up possibility for exploiting nonlinear response in optical materials.

Indeed, just a year after the laser invention, in 1961 Franken demonstrated second harmonic generation (SHG) in quartz [6]. It was estimated that about 10^{11} second-harmonic photons were generated in that first experiment from 3 J of input free-running ruby laser pulse, giving a conversion efficiency of about 10^{-8} . This experiment marked the birth of the field of nonlinear optics which complemented very fruitfully the technology development of lasers. By employing upconversion and downconversion processes, the wavelength ranges unreachable by laser sources became available for different applications. Moreover, the nonlinear optical interactions later become recognized as key for ultrashort pulse generation in bulk and fiber lasers. The low efficiency issue had been solved very quickly. In 1962 papers by Giordmain [7], and Maker et al. [8] published in the same issue of Physical Review Letters pointed out the need for phase matching and demonstrated birefringence phase-matching in KDP. The paper by P.D. Maker contains the first demonstration of what has become known as the Maker fringe technique used to this day for characterizing second-order nonlinear coefficients in new nonlinear materials. A rigorous theoretical development was in works at the same time at Harvard University. The seminal paper by J.A. Armstrong and coworkers which was published the same 1962 year provided a very detailed theoretical framework of nonlinear interactions of electromagnetic waves in dielectric media [9]. There, accurate solutions of the CWE for three-wave mixing in the plane wave approximation have been obtained. G.D. Boyd and D.A. Kleinman extended the theory to interactions for more realistic focused Gaussian beams in 1968 [10].

From the start, the experiments in nonlinear optics were limited by the obvious requirements of phase matching and high intensity

* Corresponding author.

E-mail address: vp@laserphysics.kth.se (V. Pasiskevicius).

in order to harness the nonlinear polarization contributions. Initial experiments were carried out using crystalline quartz and KH_2PO_4 (KDP) as the nonlinear media. Both materials have good transparency in the region of the second harmonic of ruby laser; however, it was clear that the low nonlinearity and dispersion would limit the application range of these materials. This problem was appreciated from the very beginning of nonlinear optics. Armstrong et al. in Ref. [9] already proposed several methods which would allow an increased effective nonlinear interaction length in the crystals with non-perfect phase matching. The idea hinges on periodic re-setting of the nonlinear interaction phase as will be explained in more detail in the next section. The proposed methods and their later variants are now collectively called quasi-phase matching (QPM) techniques.

Over the past 50 years a large number of second-order nonlinear crystals have been synthesized and demonstrated [11,12]. The prolific bibliography of nonlinear crystals is somewhat misleading however, as the large part of the synthesized crystals have never reached beyond the simple characterization stage. One can define a figure of merit for second-order nonlinear crystal as $\text{FOM} = I_d d_{\text{eff}}^2 / n^3$, where I_d is the optical damage intensity, d_{eff} is the effective nonlinear coefficient and n is the index of refraction. This definition is somewhat arbitrary because the optical damage intensity is a function of operation conditions such as pulse-length, average power and wavelength but, nevertheless, it can serve as a good guide for initial crystal selection. Even if FOM is large for certain crystal, other consideration can prevent it from being adopted for applications, for instance the difficulty of growing to large-volume, toxicity of the growth process, etc. As a result, after 50 years there are only a few crystals, specifically those which allowed birefringence phase matching for upconversion or downconversion using standard lasers based on rare-earth ions and Ti:Sapphire that have reached commercialization stage. Although the following list is not exhaustive, we can identify ten birefringence phase matched crystals, namely, KDP, β - BaB_2O_4 (BBO) [13], LiB_3O_5 (LBO) [14], $\text{CsLiB}_6\text{O}_{10}$ (CLBO) [15], BiB_3O_6 (BiBO) [16], $\text{MgO}:\text{LiNbO}_3$ [17–20], KTiOPO_4 (KTP) [21], ZnGeP_2 (ZGP) [22,23], CdSiP_2 (CSP) [24], DAST [25,26] which have found or are expected to find their application niches.

Usually, the selection of particular crystal entails compromise of the above-mentioned physical, technological and economic constraints. For instance, KDP and its isomorph DKDP have a rather low nonlinearity of $d_{36} = 0.39 \text{ pm/V}$ [11] and are hygroscopic, but they have excellent transmission properties and they can be grown to very large crystal sizes suitable for inertial fusion systems [27]. Another example of the application-driven crystal development is found in the family of borates. Here CLBO crystal was developed with the view of the optical lithography roadmap which required shifting the wavelength of the optical lithography sources down to 193 nm [28]. CLBO was promising due to possibility of phase matching below 200 nm, substantially lower Poynting vector walk-off than in BBO and a potential for growth of large crystal sizes [15]. Indeed all-solid-state systems have been demonstrated [29,30] but at present it is hard to see them competing in terms of energy, and average power with more established ArF excimer lasers. Probably the most important lesson that the nonlinear optical materials community had to learn over the past two decades is the economic one. Due to a long development and technology refinement time with associated expenses it takes a very strong argument of strategic applications with a long-term horizon in order to motivate an effort in new crystal development. One of such instances might be the development of organic DAST and semiconductor CSP crystals motivated by the requirements for high-power tunable mid-infrared and far-infrared coherent sources [24,31].

However, the picture above is not complete until we consider the nonlinear media employing the QPM principles. There are

two points which we hope to prove, at least in part, in this article. First, the QPM technique provides additional degrees of freedom allowing design of spatial and temporal properties of nonlinear interactions. Second, the additional capabilities afforded by the QPM techniques shifted focus in the field of nonlinear materials from the synthesis of new crystals with specific phase matching and nonlinear properties towards the engineering of nonlinear interactions and refining materials which can take advantage of the QPM techniques. This shift was gradually happening over the last 20 years. The result of this development is something which can be thought of as a nonlinear optics engineering toolbox which could be added to the existing and developing laser engineering methods. Although this shift occurring in the nonlinear optical materials field is not nearly as dramatic and disruptive as the invention of the laser 50 years ago, its importance should not be underestimated.

In the following sections we will briefly outline the principles, advantages and problems associated with structured nonlinear media as well as current development status of QPM materials. It is our view that the future advances in applications of QPM media will depend in a crucial way on further efforts in material research which could address specific issues related to the reliability, the lifetime, scaling to larger energies as well as addressing the structuring technology itself.

2. How QPM can work for you

As mentioned above, the QPM principle has been introduced in 1962 by Armstrong and co-workers [9]. The idea is in principle very simple. Inspection of the coupled wave equations (CWE) governing three-wave mixing (TWM), the lowest-order nonlinear processes, satisfying the energy conservation relation

$$\omega_1 = \omega_2 + \omega_3, \quad (1)$$

shows that the generated field intensity integrated over the interaction area will be very low unless the momentum conservation condition

$$\Delta \mathbf{k} = \mathbf{k}_1 - \mathbf{k}_2 - \mathbf{k}_3 = 0, \quad (2)$$

is also satisfied. Indeed, for each propagation length, equal to the coherence length $l_c = \pi / |\Delta \mathbf{k}|$ the phase difference of π is accumulated by the interaction and the TWM process reverses its direction. By adding a phase shift of π periodically every coherence length, the field intensity of the generated wave(s) will keep increasing. This can be achieved by several methods including periodic total internal reflection, periodic propagation over dispersive phase-slip regions, or periodic inversion of the sign of the second-order nonlinear coefficient [9]. The simplest QPM method is based on employing the phase shift due to a periodic total internal reflection. It has been demonstrated first in 1966 by frequency doubling of a CO_2 laser in plane-parallel slabs of GaAs and ZnSe [32]. The method was also revisited later [33,34]. Although the method is simple, it has two drawbacks. First, the number of reflections is limited due to the surface scattering losses and the beam separation owing to Goos-Hänchen shift at the boundary [35]. Second drawback is that the possibilities for interaction engineering are limited. A substantially more versatile technique to introduce the required phase shift is by spatially structuring the second-order nonlinearity. This can be achieved by different methods as will be overviewed in the following section.

For the sake of completeness and in order to give a better understanding of the QPM design principles we provide here a brief theoretical description of the second-order interaction in media with spatially structured second-order nonlinear coefficient $d_{ij} = \chi_{ikl}^{(2)} / 2$ where $\chi_{ikl}^{(2)}$ is the second-order susceptibility tensor. The TWM of Eq.

(1) is described by the CWE, which, in the slowly varying envelope approximation for monochromatic plane waves can be written:

$$\begin{aligned} \mathbf{k}_1 \cdot \nabla E_1 &= -i \frac{\omega_1^2}{c^2} d_{ij} E_2 E_3 \exp(i\Delta \mathbf{k} \cdot \mathbf{r}), \\ \mathbf{k}_2 \cdot \nabla E_2 &= -i \frac{\omega_2^2}{c^2} d_{ij} E_1 E_3^* \exp(-i\Delta \mathbf{k} \cdot \mathbf{r}), \\ \mathbf{k}_3 \cdot \nabla E_3 &= -i \frac{\omega_3^2}{c^2} d_{ij} E_1 E_2^* \exp(-i\Delta \mathbf{k} \cdot \mathbf{r}), \end{aligned} \quad (3)$$

where c is speed of light in vacuum and \mathbf{r} is the spatial coordinate. For simplicity, consider a process where two waves are much stronger than the third one and assume that depletion is not important. Then Eq. (3) simplifies to a single equation. Consider a sum-frequency mixing (SFM) process (Eq. (1)) in a medium which contains one-dimensional (1D) structure of nonlinear coefficient distributed along the x -axis coinciding with the direction of wave-vectors, $d(x) = d_{ij}g(x)$, where $g(x)$ can take values of ± 1 inside the nonlinear medium and is zero elsewhere. Analysis of a periodic 1D structure of this kind has been done in Ref. [36]. In general, integrating the first equation in Eq. (3) over the length L gives:

$$E_1(L) = -i \frac{\omega_1}{n_1 c} d_{ij} E_2 E_3 \int_{-\infty}^{\infty} g(x) \exp(i\Delta k x) dx. \quad (4)$$

It is clear from Eq. (4) that the field magnitude at the sum frequency will be proportional to the Fourier transform of the spatial distribution of the nonlinear coefficient. If the crystal is homogeneous, i.e. $g(x) = 1$, for $-L/2 \leq x \leq L/2$, it is straightforward to see that the field at SFM frequency at the end of the crystal will be

$$E_1(L) = -i \frac{\omega_1}{n_1 c} d_{ij} E_2 E_3 L \text{sinc}(\Delta k L / 2), \quad (5)$$

where $\text{sinc}(x) = \sin(x)/x$. The intensity of the generated SFM wave then is

$$I_1(L) = \frac{2\omega_1^2}{n_1 n_2 n_3 c^3 \epsilon_0} d_{ij}^2 I_2 I_3 L^2 \text{sinc}^2(\Delta k L / 2), \quad (6)$$

where ϵ_0 is the permittivity of free space. Consider a 1D structure containing periodic modulation of the sign of nonlinear coefficient with a period of Λ and a duty cycle, $D = l/\Lambda$, where l is the length within the period containing nonlinear coefficient of the same sign. By approximating this periodic modulation of $g(x)$ with discrete Fourier series:

$$g(x) = \sum_{m=-\infty}^{\infty} G_m \exp(-iK_m x), \quad (7)$$

the Eq. (4) becomes

$$E_1(L) = -i \frac{\omega_1}{n_1 c} d_{ij} E_2 E_3 \sum_{m=-\infty}^{\infty} G_m \int_{-\infty}^{\infty} \exp(i(\Delta k - K_m)x) dx. \quad (8)$$

Apart from the nonlinear dependence on the field strength, the Eq. (8) is formally analogous to the problem of X-ray scattering in crystals with the Fourier coefficients

$$G_m = \frac{2}{\pi m} \sin(\pi D m), \quad (9)$$

corresponding to the electron-cloud scattering form-factors and the structure wavevector

$$K_m = \frac{2\pi m}{\Lambda}, \quad (10)$$

corresponding to the reciprocal lattice vector in crystals. Indeed the mathematical treatment and theoretical design methods for structured nonlinear crystals is essentially borrowed from the field of solid-state physics. For a given process with frequencies of the interacting waves varying only slightly around their central

frequencies ω_2, ω_3 it is possible to find a single reciprocal vector K_m which would maximize the output at ω_1 . Namely, the structure should be designed to satisfy the QPM condition $\Delta k = K_m$ preferably using the first order QPM ($m = 1$) as this also maximizes the Fourier coefficient in Eq. (9). The SFM intensity at the end of the QPM structure can be expressed as:

$$I_1(L) = \frac{2\omega_1^2}{n_1 n_2 n_3 c^3 \epsilon_0} d_{ij}^2 \left(\frac{2}{\pi m} \right)^2 \sin^2(\pi m D) I_2 I_3 L^2 \text{sinc}^2((\Delta k - K_m)L/2). \quad (11)$$

It is evident that the QPM interaction is formally analogous to the birefringence phase matched process (Eq. (6)), however, with the nonlinear coefficient reduced by a factor of $(2/(\pi m)) \sin(\pi m D)$. It should be stressed that the benefits offered by having an additional design parameter K_m in most cases far outweighs the drawback of the reduced nonlinear response for QPM structures. Let us specify some of those benefits: (1) QPM structures can be designed for any TWM interaction within the transparency region of a particular crystal, regardless of the birefringence properties. (2) It is often the case that diagonal susceptibility tensor elements are the largest ones, but they cannot be utilized by employing birefringence phase matching. For example, in KTP the nonlinear coefficient employed in birefringence phase matched TWM is $d_{24} = 3.75$ pm/V. In QPM structures fabricated in KTP one can exploit the nonlinear coefficient $d_{33} = 15.4$ pm/V [37] thus giving almost 7-times larger efficiency for the same crystal length. This possibility to use substantially higher nonlinearity allowed demonstrations of CW-laser and even laser diode-pumped singly-resonant optical parametric oscillators (OPOs) [38–41]. (3) Due to the fact that one does not need to care about birefringence phase matching, the propagation directions of the waves in QPM structure can be chosen to coincide with one of the indicatrix axes. This eliminates Poynting vector walk-off, which normally limits the usable crystal length in birefringence phase matched interactions.

Periodic modulation of the nonlinear susceptibility with a duty cycle of 0.5 will maximize the Fourier component of the required value of Δk and will result in the maximum conversion efficiency for the first QPM order. However, even if the structure is not perfect or even random the TWM efficiency will be higher than in a homogeneous non-phase-matched crystal [42,43]. Indeed, consider the TWM process in a homogeneous crystal with a large Δk . In this case the largest part of the power after the crystal will be generated over the last coherence length, $\pi/\Delta k$. If the crystal contains a random structure of the second-order susceptibility, the generated power at ω_1 will increase linearly in proportion to the number of domains encountered by the input beams (ω_2, ω_3) [42,43]. Fig. 1 shows a comparison of the calculated dependence of the SHG efficiency as a function of normalized crystal length for the first order QPM ($m = 1, \Delta k = K_1$), the fifth-order QPM ($m = 5, \Delta k = K_5$), for a homogeneous crystal with large phase mismatch and for a crystal containing a random structure of nonlinear coefficient where the domain sizes are distributed by Poisson distribution with the mean domain length of $4 \mu\text{m}$ and the variance of $4 \mu\text{m}$. The fundamental wavelength here is $1 \mu\text{m}$ and the crystal length is normalized to the nonlinear interaction length, $L_{nl} = n_1 c / (\omega_1 d_{ij} E_2)$. Enhancement of the conversion efficiency by the presence of a random structure is evident. The random structure might even give higher efficiency than higher-order QPM structure if the crystal length is limited.

Potentially higher efficiency gained by employing QPM structures is obviously interesting for applications, especially those using frequency conversion of CW and low power laser sources. However, probably the strongest argument for using QPM technology is that it gives possibilities to add functionality to the nonlinear

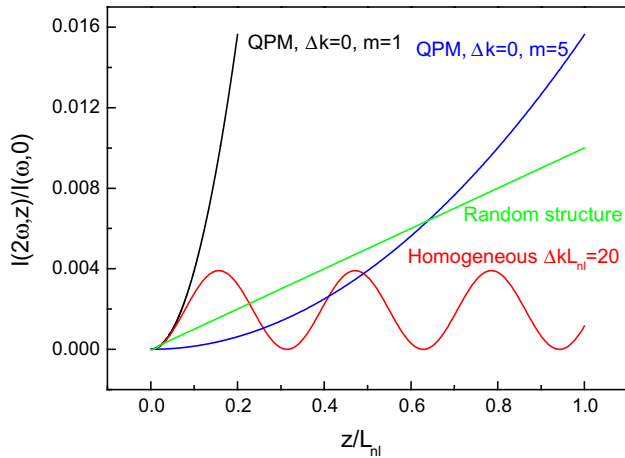


Fig. 1. Calculated efficiency in nondepletion approximation as a function of normalized structure length. Perfectly phase-matched first order QPM (black line), phase-matched 5th order QPM (blue line), structure with random modulation of the nonlinear coefficient sign (green line), and non-phase-matched homogeneous crystal (red line). (For interpretation of the references to colour in this figure legend, the reader is referred to the web version of this article.)

process which is otherwise not possible to obtain using standard birefringence phase matching.

The first demonstration of tunable optical parametric frequency converter with QPM structures involved multi-period gratings fabricated on a single chip [44]. Later on a fan-out grating design has been proposed by P.E. Powers and co-workers to achieve continuous tuning of the output wavelength by lateral translation of the nonlinear crystal [45]. The continuous tunability of a parametric oscillator using noncollinear interactions have been later demonstrated in simple single-period QPM structures [46,47]. Spectral shaping of nonlinear interactions is an important tool for frequency conversion of ultrashort pulses and for generation of widely tunable coherent radiation. The design procedure can be easily derived by considering pulses at central frequencies $\omega_1, \omega_2, \omega_3$ travelling with their associated group velocities as given in Eq. (3). For simplicity, considering the second harmonic process, $\omega_2 = \omega_3$, and by introducing a coordinate frame moving with the group velocity v_{g1} of pulse E_1 , i.e. $\tau = t - x/v_{g1}$, the Eq. (4) can be transformed into the form

$$E_1(L, \tau) = -i \frac{\omega_1}{n_1 c} \frac{d_{ij}}{\delta} \int_{-\infty}^{\infty} E_2^2(\tau - \tau') g(\tau') \exp(i\Delta k \tau' / \delta) d\tau', \quad (12)$$

where $\delta = v_{g2}^{-1} - v_{g1}^{-1}$ is the group velocity mismatch and $\tau' = x\delta$. The Eq. (12) contains a convolution integral, which directly tells us that the spectrum of the second harmonic pulse will be equal to the product of the Fourier spectrum of the square of the fundamental pulse field and the Fourier spectrum of the QPM structure using τ' as a time basis. By making the QPM structure with varying periodicity not only a broad spectral bandwidth can be generated but also the generation process itself in such structures can be used for pulse compression or pulse stretching [48–52]. For broadband parametric gain shaping is also possible to employ noncollinear interactions which are often used in birefringence phase matched TWM processes, with the added advantage in the QPM case, that the spectral wavelength range can be easily tailored to suit the application [53–55].

The flexibility offered by the additional design parameter K_m (Eq. (8)) can be exploited in a straightforward way for quasi-phase matching several processes in the same 1D structure. Indeed a structure should simultaneously compensate for the phase mismatch in any number N of TWM processes if it's Fourier spectrum contains appropriate reciprocal vectors $K_{mj} = (\Delta k)_j, j = 1 \dots N$. This

flexibility has been exploited using several different designs [56–59]. The Fourier components of the QPM spectrum can be added by modulating periodicity of the structure. However, in order to maximize the efficiency only in the TWM processes of interest the Fourier spectrum ideally should contain only the needed reciprocal vectors and not the quasi-continuous distribution of Fourier components. That essentially means that the modulation function should be non-differentiable. The generalized procedure of such quasi-periodic QPM structure design, borrowed from the field of crystallography has been outlined in Ref. [60] and later experimentally demonstrated [59]. Moreover it has been proven that the efficiency of multiple TWM processes in a quasi-periodic structure is substantially higher than could be achieved in the same length of the crystal containing composite periodic QPM gratings.

The special case of multiple processes occurring during a second-order interaction is the degenerate or close to degenerate cascading of a frequency doubling followed by a downconversion. It is well known that $\chi^{(2)}:\chi^{(2)}$ cascading emulates a third-order nonlinear response and can produce large intensity-dependent phase shifts [61]. Obviously, this process happens also in birefringence phase-matched materials, however due to much larger $\chi^{(2)}$ nonlinearity accessible in QPM crystals, the effective third order nonlinearity due to cascading is also substantially higher in this case. Moreover, the QPM structures can be designed specifically for enhancement of cascading [62]. Specific QPM structure designs have been proposed for shaping quadratic spatial solitons [63] and such solitons have also been experimentally observed [64]. A Kerr lens obtained through the cascaded interactions was also utilized for passive mode-locking of solid-state lasers [65,66]. Near-degenerate cascaded processes are equivalent to four-wave mixing (FWM) parametric interactions occurring in the third-order media. FWM processes are interesting for applications in all-optical wavelength converters (AOWC), required by high-capacity optical communications systems. One example of such cascaded FWM in a periodically-poled KTP (PPKTP) is shown in Fig. 2. Here the narrow cascaded sidebands are generated in a narrowband (OPO) [67]. For instance, generation of the first signal sideband involves two $\chi^{(2)}$ processes $\omega_{s1} = \omega_s + \omega_s - \omega_i$, etc. Recently, a polarization-insensitive cascaded FWM AOWC scheme using periodically-poled LiNbO₃ (PPLN) waveguides has been demonstrated at 100 Gb/s capacity [68].

Optimization of the FWM parametric gain spectrum is also possible due to the capability to engineer the QPM structure. For instance, by taking inspiration from well-developed techniques of fiber Bragg gratings, an apodized QPM structure has been proposed and demonstrated in PPLN [69]. Owing to the tapering of the domain duty cycle, the flat and ripple-free gain spectrum can be produced.

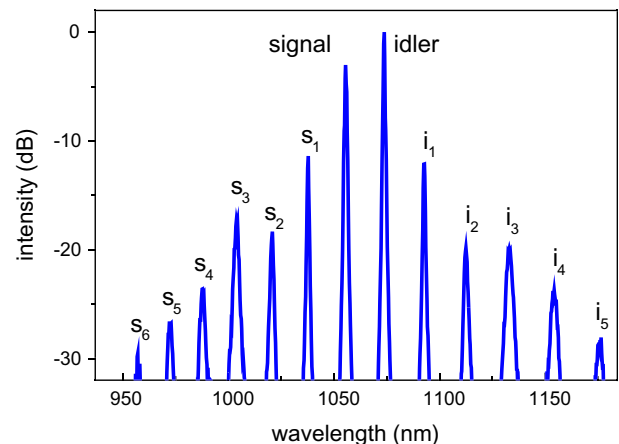


Fig. 2. Cascaded $\chi^{(2)}:\chi^{(2)}$ FWM spectrum in a near degenerate interaction.

Over the last decade the structuring technologies in different second-order nonlinear materials achieved finesse high enough to start demonstrating nonlinear processes and devices which are impossible in homogeneous media. This trend of synthesizing new “reality” is bound to continue into the future and it indicates stronger that anything told so far that the whole nonlinear optics field has moved into the realm of engineering. Currently, to the list of novel devices enabled by the QPM techniques we can put devices employing counter-propagating TWM, backward-wave oscillators and nonlinear photonic crystals (NPC).

Consider a Bragg reflector whose reflectivity and spectrum can be externally modulated. This can be achieved if the Bragg reflector consists of an electro-optic material with periodically structured electro-optic coefficient. The periodicity of the structure, $A_m = m\lambda/2n$, where n is the index of refraction, should be about a quarter of the wavelength in vacuum for the first order reflection. It is a challenging technological task to fabricate such structures as will be discussed in the next section. Nevertheless, the spectrally selective Bragg reflector operating at the third order of diffraction has been demonstrated in a PPKTP structure with a domain periodicity of 800 nm [70]. Backward SHG is another process which requires a sub-wavelength periodicity of the QPM structure as can be seen from the vector diagram in Fig. 3, namely, $A_m = m\lambda/(2(n_{\omega} + n_{2\omega}))$. SHG at higher orders (down to 16th) has been demonstrated in PPLN and PPKTP waveguides using pulsed pumping [71,72]. CW backward SHG at 7th order has been obtained in a bulk PPKTP structure with a period of 720 nm, as can be seen in the phase matching spectrum in Fig. 4 [73]. One of the striking features of a counter-propagating interaction is the high temporal coherence of the backwards generated wave. For instance, the SHG phase matching bandwidth for the quasi-CW excitation in the structure of length L can be expressed as

$$\Delta\lambda = \frac{0.443\lambda^2}{L(n_{g1} \pm n_{g2})}, \quad (13)$$

where λ is the fundamental wavelength, n_{g1} and n_{g2} are the fundamental and the second harmonic group indices, respectively. For the backward SHG bandwidth one has to take the plus sign in the denominator, which immediately tells us that the bandwidth for the counter-propagating case will be at least order of magnitude smaller than in the usual, co-propagating SHG.

The wave-vector diagrams for the collinear optical parametric interactions are shown in Fig. 5, where the case for co-propagating optical parametric generation (OPG), Fig. 5a is compared with three possible counter-propagating cases Fig. 5b–d. To give an example of the required structures to achieve these interactions, in Fig. 6 we present the calculated QPM period as a function of the quasi-phase matched parametric signal wavelength for all three counter-propagating geometries. The calculation was done for PPKTP and it was assumed that the pump wavelength is 822 nm. As can be seen from the Fig. 6, all these processes require QPM structures with sub-micrometer periodicity fabricated over a length on the about 1 cm or more in order to keep the generation

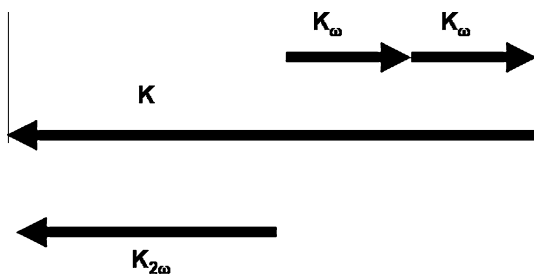


Fig. 3. Wave vector diagram for backward SHG.

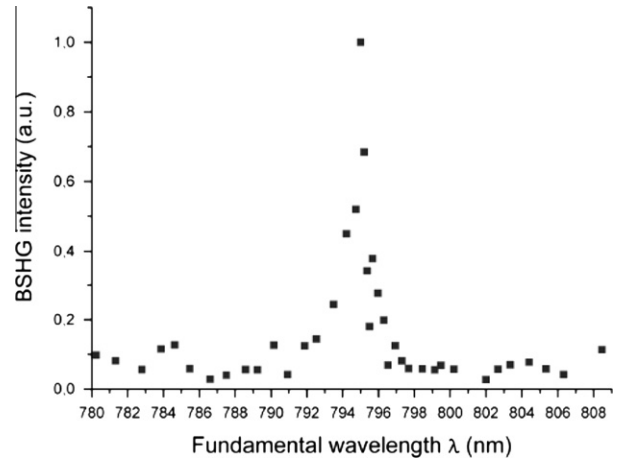


Fig. 4. Backward CW SHG phase matching spectrum generated with a bulk PPKTP structure containing a 720 nm periodicity.

threshold comfortably far from the optical damage threshold. If one of the waves, the signal or the idler, are counter-propagating then it is possible to obtain a mirrorless oscillation due to the automatically-established distributed feedback, schematically illustrated in Fig. 7, for the case of the idler-counter-propagating mirrorless optical parametric oscillator (MOPO). The MOPO was theoretically proposed already in 1966 in Ref. [74], where it was also emphasized that the birefringence in homogeneous second-order crystals is not large enough to realize this device. Instead, the MOPO has been demonstrated in QPM structures [75,76], and it took 31 year for the structuring technology to achieve the required level of precision and to reach a sophistication where this was possible. Counter-propagating parametric interactions offer rather unique spectral properties as well. It is notoriously difficult to obtain a narrowband spectrum in mid-infrared using standard co-propagating OPOs, especially when operating close to degeneracy. This statement is especially true for the QPM OPOs using periodically poled KTP, LiNbO₃ or LiTaO₃, which employ signal and idler waves of the same polarization, in order to take advantage of the largest nonlinear coefficient. It is instructive to compare the MOPO spectrum with the spectrum of a co-propagating PPKTP OPG pumped by picosecond pulses at the same wavelength as the MOPO, and generating signal and idler in the same spectral region. For the co-propagating OPG we used PPKTP with a QPM period of 28.5 μm. The comparison of the signal spectra generated in the MOPO and the co-propagating OPG can be seen in Fig. 8. Here, the co-propagating OPG generates a signal with a FWHM spectral width of 32.7 THz. The material dispersion characteristics are being the same for the MOPO, nevertheless it generates a signal with a spectral width which is only 270 GHz. Furthermore, the MOPO idler is more than an order of magnitude narrower than the signal, less than 23 GHz, as verified in the measurement limited by the resolution of the spectrometer.

The structuring of the second-order nonlinearity does not need to be only one-dimensional. The structuring technology which is based on a planar lithography allows straightforward extension of the QPM principles into a 2D case. Theoretically such structures, also called nonlinear photonic crystals, were proposed by Berger in 1998 [77]. Indeed the solutions of CWE, (see Eq. (3)) by extending the TWM solution of Eq. (8) to a 2D case, can be written [53]:

$$E_1 = -i \frac{\omega_1}{n_1 c} \frac{d_{ij}}{w} E_2 E_3 \iint_{-\infty}^{\infty} g(\mathbf{r}) \exp(i\Delta\mathbf{k} \cdot \mathbf{r}) \cdot dxdy, \quad (14)$$

where w is the width of the interaction area. The modulation function, $g(\mathbf{r})$, is composed of three parts, a 2D mesh of delta functions describing the periodic pattern which is convoluted with a motif

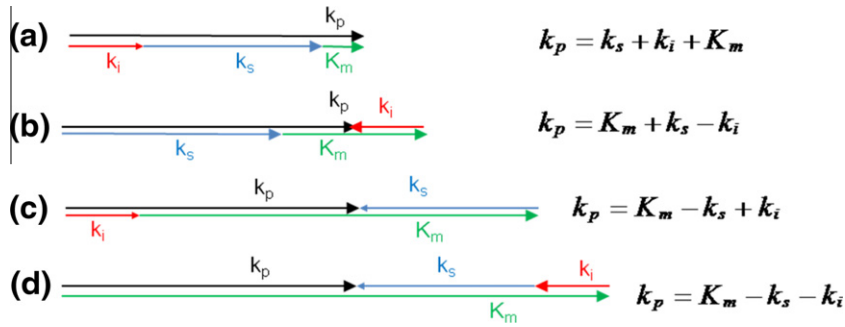


Fig. 5. Quasi-phase matching wavevector diagrams and momentum conservation relations corresponding to the collinear optical parametric interactions. Co-propagating (a), idler counter-propagating (b), signal counter-propagating (c), signal and idler counter-propagating (d) interactions.

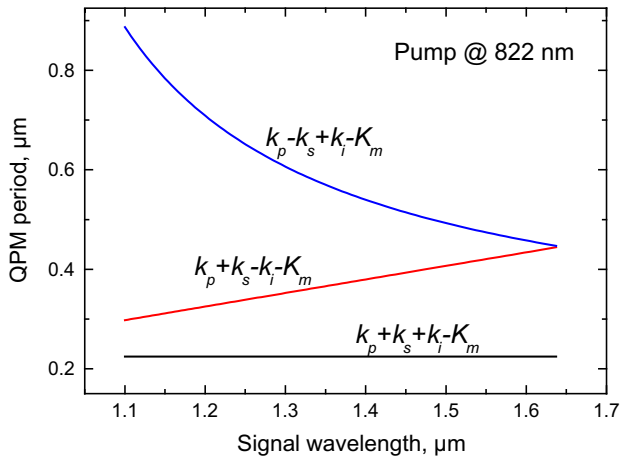


Fig. 6. Calculated QPM periodicity required for phase matching counter-propagating parametric interaction in PPKTP as a function of signal wavelength at a fixed pump wavelength of 822 nm. Counter-propagating idler (blue line), counter-propagating signal (red line), and counter-propagating signal and idler (black line). (For interpretation of the references to colour in this figure legend, the reader is referred to the web version of this article.)

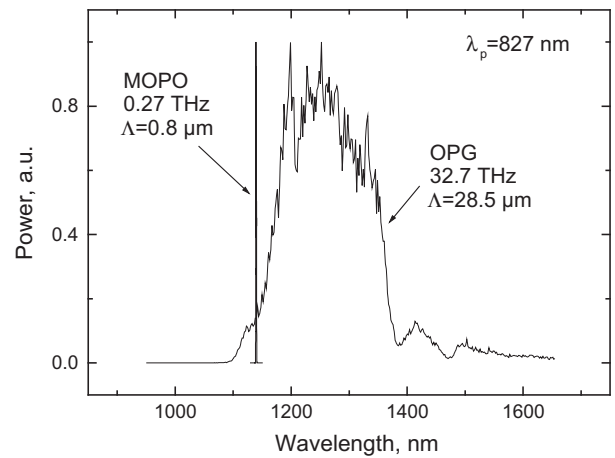


Fig. 8. Comparison of spectral bandwidths generated for a co-propagating optical parametric (OPG) generator and a MOPO with counter-propagating idler. Both devices were realized with PPKTP with periodicity of 28.5 μm and 800 nm used for OPG and MOPO, respectively. Both devices are pumped at the same conditions. The MOPO idler was narrower than 23 GHz or a three-orders of magnitude narrower than for the ordinary OPG.

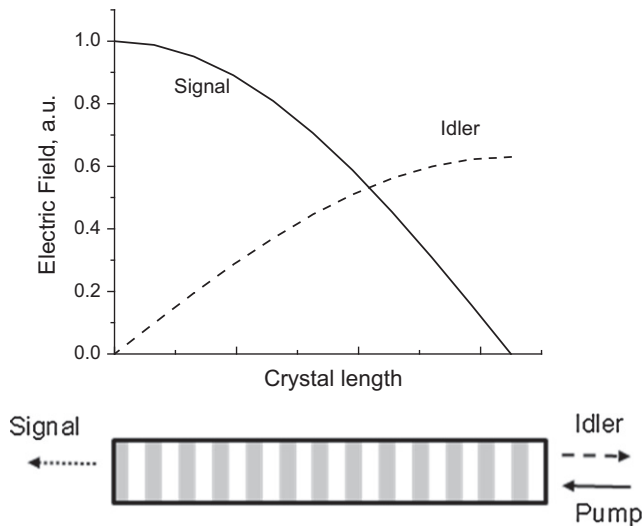


Fig. 7. Geometry and normalized electric field amplitude distribution for a mirrorless OPO with counter-propagating idler.

function describing the geometry of the domain centered at each real space grating nod and multiplied by an interaction area function. Therefore, as in the 1D case, the Eq. (14) tells us that the SFM electric field amplitude will be proportional to the Fourier

transform (2D) of the nonlinearity modulation function. For some geometries, such as those containing periodic patterns of rectangular or circular motifs it is possible to find analytic solutions [78]. The NPC was first demonstrated in LiNbO_3 2D-periodically poled with hexagonal pattern (HexLN) [79]. An example of a 2D periodically poled KTP with a rectangular lattice periodicity of 6 μm is shown in Fig. 9 [80]. Here, the polar surface of the crystal has been etched to reveal domains with opposite signs of the second-order nonlinearity. Exactly as in solid-state physics one can construct a reciprocal lattice orthogonal to the real-space lattice, $(\mathbf{a}_x, \mathbf{a}_y)$, such that $\mathbf{a}_i \cdot \mathbf{K}_j = 2\pi\delta_{ij}$. Quasi-phase matching for a TW process will be achieved in the directions where the phase mismatch is compensated by a linear combination of the reciprocal lattice vectors as shown in Fig. 10:

$$\Delta\mathbf{k} = \mathbf{k}_{2\omega} - 2\mathbf{k}_\omega = \mathbf{K}_{mn} = m\mathbf{K}_{10} + n\mathbf{K}_{01}. \quad (15)$$

The theoretical and the experimental mapping of the reciprocal lattice vectors in the above-described 2D PPKTP is demonstrated in Fig. 11 for the SHG process at the fundamental wavelength of 946 nm.

The capability to structure nonlinearity in 2D opens up some very interesting possibilities for shaping spectral and spatial beam properties in TW. And the pattern does not need to comprise a 2D lattice. Interesting examples here can be Airy beam generation in TW where the pattern consists of a periodic stack of cubic functions [81] or Bessel beams which can be generated in the

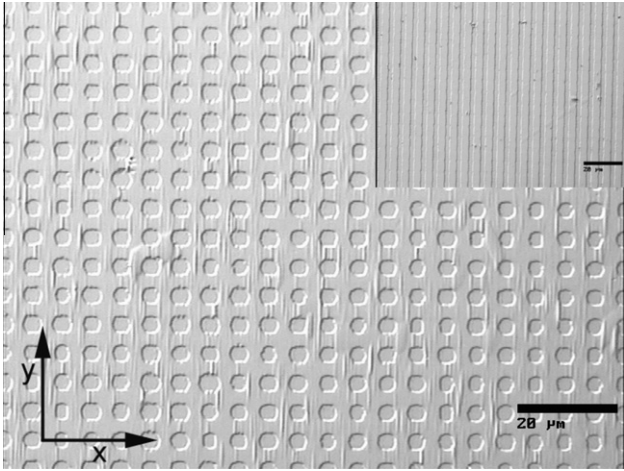


Fig. 9. Rectangular pattern in a 2D-poled KTP with a periodicity of 6 μm. The inset shows the usual 1D pattern in PPKTP.

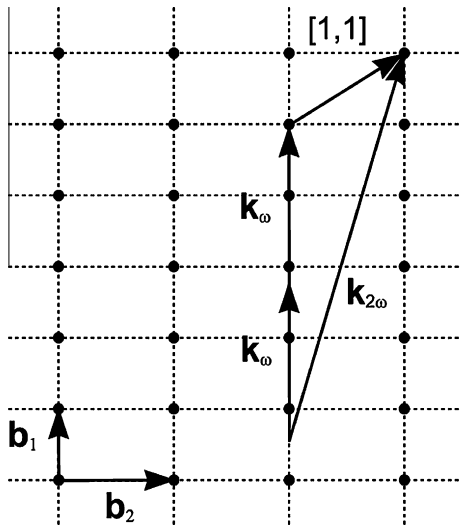


Fig. 10. Reciprocal lattice for a rectangular real-space lattice. The case of quasi-phase matching of SHG by using the reciprocal lattice vector \mathbf{K}_{11} .

nonlinear structure consisting of periodic concentric rings [82]. There is no doubt that the demonstrations of this novel functionality in 2D-structured nonlinear media will continue in the future.

3. Progress in QPM materials

Early attempts to employ artificially structured nonlinearity for enhancement of TWM interactions was by using stacked plates of a nonlinear material where adjacent layers are rotated by 180 degrees to give a sign reversal in $\chi^{(2)}$. This QPM method was demonstrated in nominally non-birefringent semiconductors CdTe [83] and GaAs [84,85] as well as crystalline quartz, LiNbO₃ [86] and LBO [87]. Clearly, the QPM structure consisting of stacked plates, introduces additional losses due to multiple Fresnel reflections. Integration of the plates into a monolithic stack was later achieved by diffusion bonding the rotated plates of GaP [88] as well as GaAs [89]. The stacking and bonding process requires some extensive effort in plate preparation in order to get homogeneous bonding contact across the plates. Moreover, it is difficult to extend this technique for structures operating in the mid-infrared spectral range as the thickness of the plates becomes smaller than

100 μm. Consequently, the applications of this technique was and will probably be in the far infrared and the THz spectral ranges.

Economic aspects are very important in the development new materials and in broadening the range of applications of nonlinear media. In this respect, the QPM media are not different from the birefringence phase matched crystals. Therefore, it is not surprising that a huge activity increase in the field of QPM devices which we witnessed over the past 15 years came after the technologies amenable for mass-fabrication and planar wafer processing were demonstrated in commercially available nonlinear crystals with high nonlinearities and relatively high damage thresholds.

Periodic inversion of spontaneous polarization domains in ferroelectrics proved to be such enabling technology. Ferroelectrics and their domain structures were investigated long before the invention of the laser. The research in piezoelectric properties of such crystals as Rochelle salt, KDP [90], LiNbO₃ [17], BaTiO₃ [91] was active in the 1950s. The early research, mostly at Bell labs, focused on piezoelectric properties of such crystals. Manipulation of the domain structures by annealing and electric field poling in KDP and BaTiO₃ [90,92] was also investigated in the piezoelectric context. Thus, by the time the QPM concept was proposed in 1962, there already existed a large body of material research data on some ferroelectrics including the possible methods of ferroelectric domain structuring. It might be puzzling, why it took to 1980s for the nonlinear optics community to start seriously exploiting the benefits of the QPM technology in ferroelectric crystals. Probably there is no single and simple answer, but a combination of factors, which prevented earlier development of such materials. Such factors might have been a lack of perceived need for more efficient nonlinear media, a slow and expensive development of high- and reproducible quality ferroelectric crystals, and the associated lack of knowledge of the dispersion data, crucial for any QPM design. An important breakthrough came when it was demonstrated that LiNbO₃ boules with periodically inverted domains and with well-controlled periodicity could be produced directly during Czochralsky growth by keeping the growing crystal at an angle with respect to the temperature field resulting in a sinusoidal variation in segregation coefficient of the dopant, Y [93]. A similar procedure was later applied to LiTaO₃ [94].

Direct growth of large volumes of periodically structured nonlinear crystals might be a good proposition for mass production if the need for such mass production exists. Probably a more flexible technique of ferroelectric structuring is by using electric field poling. The technique of periodic structuring of LiTaO₃ using interdigital finger electrode pattern had already been demonstrated in the field of ultrasonic transducers [95] in 1983. Periodic poling using diffusion and thermal treatment was later studied for the fabrication of nonlinear optical waveguides in LiNbO₃ and KTP [96–98]. In 1993 Yamada et al. [99] achieved a breakthrough in small-period electric field poling in LiNbO₃ waveguides which were intended for blue light generation in the first-order QPM process. This immediately opened up the opportunity for using periodically poled LiNbO₃ (PPLN) and PPKTP waveguides for frequency conversion of low-power laser diodes. The following substantial progress resulted in demonstration of a 99% fundamental power depletion in PPLN waveguide quasi-phase-matched for SHG at the wavelength of 1552 nm [100]. Alternative techniques for PPLN waveguide fabrication including a bonding technique are currently being explored as a possible way to increase confinement in a ridge waveguide structure, to reduce losses, and to develop a generic process which could also be applied to other periodically poled materials such as periodically poled LiTaO₃ (PPLT), where the waveguide fabrication using chemical processing proved to be difficult [101]. PPKTP waveguide technology has also shown good progress [102,103] making them a choice media for generation of blue-green coherent light due to high resistance of KTP to photorefractive damage. In the longer wavelength region,

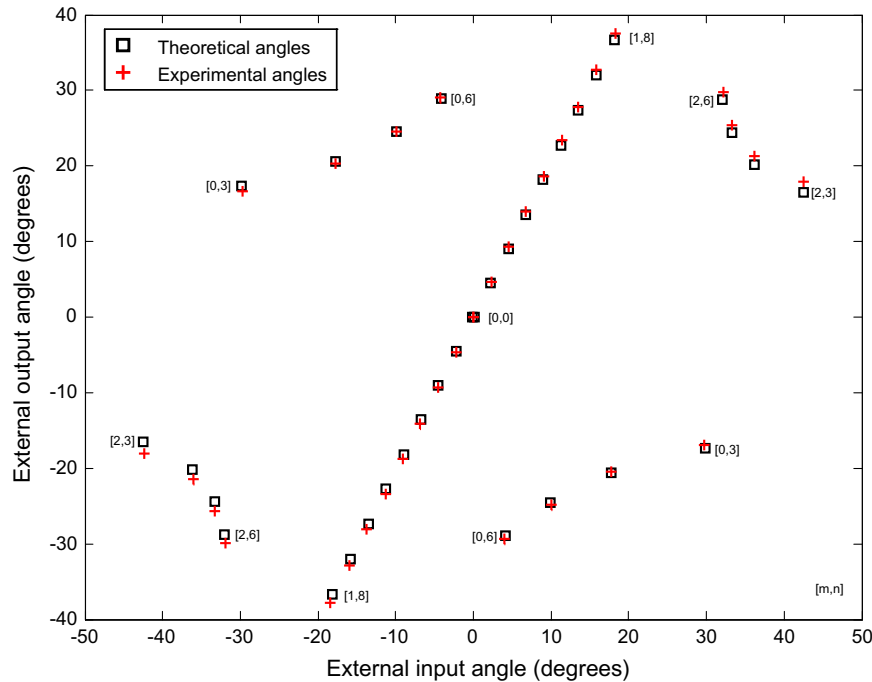


Fig. 11. The calculated (squares) and measured (circles) external output angles of the SH beam, versus the external input angle, using a 946 nm Nd:YAG laser as the fundamental source. The values in parentheses are the indices specifying the reciprocal lattice vector, \mathbf{K}_{mm} , responsible for quasi-phase matching.

a constant progress is being demonstrated in development of periodically structured semiconductor waveguides, where the normalized frequency doubling efficiencies of $21\%W^{-1}$ at the fundamental wavelength of $4\ \mu\text{m}$ and $23\%W^{-1}$ at the optical telecommunications wavelength of $1.55\ \mu\text{m}$ have been demonstrated in GaAs and AlGaAs, respectively [104,105].

Structured bulk nonlinear crystals, with all the flexibility afforded by QPM and high-power handling capability, are of great interest, indeed. In order to increase the range of applications for the QPM bulk crystals a substantial research effort is devoted towards reducing technological and material challenges. Eventually, the desired outcome is the structuring technology and the material which would allow for large optical apertures and quasi-phase matched TWM within entire transparency range which, in turn, should be as broad as possible. There are several substantial challenges on this road: (a) the material resistance to the induced optical absorption and photorefraction, which can be prominent in ferroelectrics, should be increased (b) a structuring technology which would faithfully reproduce the desired design pattern onto the $\chi^{(2)}$ structure, should be further refined, (c) the homogeneity of the initial crystal wafers which are the main determinants of the structuring success, should be increased (d) the structuring techniques should be developed for fabrication of sub-micron periodicity structures over large crystal thickness, or, in other words, the aspect ratio of the inverted domains should be increased. Some of these challenges (a, c and partly d) primarily require additional research efforts in material chemistry and material growth, the other challenges require improved methods for domain control and a better understanding of the domain inversion kinetics.

Periodic electric field poling of the bulk congruent LiNbO_3 (CLN) was reported in 1994 [106]. CLN growth at that time had been well developed so the research could focus primarily on the structuring techniques. Already in 1995 a CW laser pumped bulk PPLN OPO was demonstrated [107]. The thickness of the structures were limited to 0.5 mm due to a large coercive field in CLN ($\sim 21\ \text{kV/mm}$), which is the field required for the spontaneous polarization switching. A better understanding of the ferroelectric domain kinetics during polarization inversion was required to achieve

periodicities below $20\ \mu\text{m}$ in 0.5 mm-thick PPLN. Miller and coworkers in Ref. [108] demonstrated a substantial improvement in poling PPLN structures with sub-10 μm periodicities. A back-switching method was investigated in CLN in order to reduce the QPM periodicity even further [109]. However, so far it proved to be difficult to achieve adequate control over the ferroelectric domain kinetics in this process.

Approximately at the same time as in CLN, the electric field-poling of the bulk hydrothermally-grown KTP was demonstrated, producing QPM structures for green light generation [110]. The coercive field in KTP is an order of magnitude lower than in CLN so it is substantially simpler to fabricate QPM structures thicker than 0.5 mm. These initial demonstrations used hydrothermally-grown KTP wafers. Hydrothermal growth produced good quality homogeneous KTP crystals, but the crystal sizes were rather limited. Moreover, this growth process is very slow and has to proceed at high pressures, so, eventually, the commercial crystals were predominantly grown by a flux method. The flux-grown KTP however has high ionic conductivity due to a hopping motion of weakly bound K^+ ions and K^+ vacancies. To complicate matters further, the homogeneity of the crystal wafers depends critically on the growth conditions and can vary substantially. Nevertheless, the periodic poling techniques were developed for this material, including a Rb-exchange-assisted electric field poling [111] and a low-temperature poling [112], with both methods aiming to reduce the ionic conductivity of the commercial KTP wafers. PPKTP and its periodically poled isomorphs RbTiOAsO_4 (RTA) [113], RbTiOPO_4 (RTP) [114], KTiOAsO_4 (KTA) [115] attracted considerable attention also due to the fact that these materials did not suffer from photorefraction, as opposed to CLN, although the nonlinear coefficient, $d_{33} = 15.4\ \text{pm/V}$, in KTP [37] is almost 1.8-times lower than in CLN. As an additional advantage, KTP has a larger crystal anisotropy as compared to CLN which somewhat reduces the ferroelectric domain broadening during periodic poling, permitting rather easier scaling down of the periodicity in QPM structures to below $3\ \mu\text{m}$ [116], as well as producing homogeneous QPM structures in 3 mm-thick wafers [117]. For the fabrication of sub-micrometer-periodicity structures the poling technique in KTP

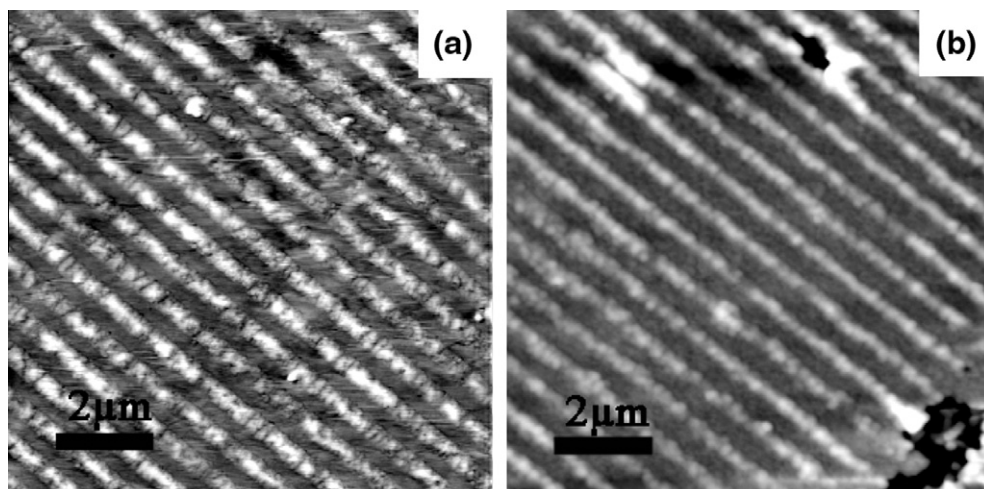


Fig. 12. AFM images showing the etched domain structure on the patterned polar surface (a), and on the backside (b). The scale bar is 2 μm .

had to be modified to further reduce the influence of fringing electric fields at the finger electrode edges. For this end, a periodic K^+ ion indiffusion from a KNO_3 melt at one of the polar surfaces proved to be very helpful [73]. Fig. 12 shows the atomic force microscope images of the periodic domain pattern with a period of 720 nm fabricated in a 1 mm-thick wafers using this technique. The aspect ratio of the domains in this structure is then 2778.

Regardless of the fast progress in structuring of the most promising QPM materials, CLN and KTP, it was evident that these crystals should be improved in order to reduce the effects of photorefractive and blue- and green-light induced infrared absorption (BLIIRA, GRIIRA) [118,119]. Previous research, which focused on CLN as a potential material for photorefractive components, revealed that doping with about 5% MgO substantially reduces photorefractive in this crystal [120]. $\text{MgO}:\text{LiNbO}_3$ was successfully poled and it was also shown that the coercive field in this material is reduced down to about 4.5 kV/cm [121]. This fact allowed fabrication of $\text{MgO}:\text{PPLN}$ structures having thickness of 5 mm and therefore allowing handling of substantial optical powers [122]. A threshold in MgO doping concentration for reduction of the photorefractive as well as reduction of GRIIRA was indeed confirmed and attributed to the reduction of native defects, Nb in Li, when Mg is incorporated on Li sites [123]. Further reduction of the coercive field in LiNbO_3 and LiTaO_3 was achieved by increasing [Li] concentration in the crystals to the extent of making them close to stoichiometric. Two methods were demonstrated to achieve this goal successfully, a double crucible Czochralsky growth [124] and a Li vapor-phase equilibration [125]. The former method might be more suitable for production of large crystal sizes and was subsequently commercialized. The, so called, near stoichiometric LiNbO_3 (SLN) and, especially, near stoichiometric LiTaO_3 (SLT), additionally doped with MgO in order to reduce photorefractive, became new materials for QPM structure fabrication using electric field poling and capable of handling substantial powers in the visible spectral range. Comparison of high-peak power BLIIRA in some of these and other candidate materials can be found in Ref. [126]. Recently, a successful periodic poling of 5-mm thick congruent LiTaO_3 heavily (7 at.%) doped with MgO has been achieved at elevated temperatures, making this material an interesting candidate for high power applications [127].

Material research efforts were required to improve performance of PPKTP as well. This material is susceptible to color center formation and a concomitant induced absorption when irradiated with high-peak power blue or green laser beams [119,126]. This is attributed to a number of possible electron and hole capture cen-

ters, and there were indications that K^+ vacancies, which are abundant in the flux grown crystals, could act as stabilizing defects. Previous material research in mixed $\text{Rb}_x\text{K}_{1-x}\text{TiOPO}_4$ crystals showed that for $x \sim 0.01\text{--}0.02$ the ionic conductivity mediated by K^+ vacancies is reduced by orders of magnitude and the material still retains similar ferroelectric properties as KTP [128–130]. Fabrication of the QPM structures indeed revealed superior properties of this solid solution crystal in terms of ferroelectric domain control as well as in terms of optical performance. High-peak power experiments revealed that the induced absorption which is present in all nonlinear crystals is drastically reduced and the absorption level does not increase in time during long term exposure [131,132]. A drastically reduced ionic conductivity in this crystal allowed fabrication of 5-mm-thick periodically poled crystals for high energy frequency conversion [133]. Another approach for increasing the aperture of the PPKTP is by template growth where the seed crystal already contains electric field-poled structure. Such template growth has been recently accomplished by employing a special composition of the flux, which permitted crystal growth substantially below Curie temperature [134].

A large progress over the last decade occurred in periodic structures fabricated in GaAs. Improving on earlier technique of stacking and bonding of GaAs plates having opposite orientations of the $\chi^{(2)}$ sign [89], two slightly different methods were developed, where an epitaxial growth over orientationally patterned GaAs (OP-GaAs) template was exploited [135,136]. The key to both methods was the availability of a fast epitaxial regrowth using hydride vapor phase epitaxy (HVPE) over GaAs template representing periodically inverted GaAs structure. This template can be produced either by molecular beam epitaxy growth of a thin Ge layer followed by an inverted layer of GaAs. Subsequent steps of lithography and chemical etching enable a very precise control over the periodicity and the duty cycle. Alternatively, the template can be produced by bonding of two GaAs plates with opposite orientations and subsequent steps of mechanical polishing, lithography and etching. Both methods produce very high quality structures and the HVPE GaAs layer shows very low absorption losses in the near infrared, lower, in fact, than that in the original GaAs substrate. OP-GaAs bulk structures with thickness exceeding 0.5 mm can be produced by these methods.

At the end of this brief overview of the progress in QPM materials we need to mention other crystals and non-crystalline media where engineering of the nonlinear interactions have been demonstrated but where the further progress will depend on advances in material research solving specific problems, and, mostly, on an application niche which is important enough to warrant required

investment in such an effort. BaTiO₃, a well-known photorefractive crystal was one of the first materials to be poled [92], but it took 40 years before OPO was demonstrated in periodically poled structure [137]. Another photorefractive crystal, Sr_{0.6}Ba_{0.4}Nb₂O₆ (SBN), was used to demonstrate quasi-phase matched SHG [138,139]. Great hopes for blue light generation were attributed to a periodically poled KNbO₃, a crystal with a complicated ferroelectric domain structure and a very interesting object from material research point of view, which, so far, proved to be too prone to self re-structuring during nonlinear interaction [140–142]. Thermally-assisted electric field poling of glass for a long time was and still remains a huge promise, having in mind applications in optical telecommunications and integrated optics [143]. There are also choices of QPM media in ultraviolet applications such as periodically poled MgBaF₄ [144] and crystalline quartz, which has been structured by applying mechanical stress [145], as well as orientationally patterned GaN [146]. In particular, the elastic-twin patterned crystalline quartz has a great promise for high-power UV generation due to a large bandgap of around 9 eV and the availability of high-quality and large-size crystals. The first UV generation by frequency doubling in the structured quartz [147] indeed shows a potential of the twin-patterning technology in this material. Deeper into XUV the QPM principles can be applied as well as was brilliantly demonstrated in high-harmonic generation in gas-filled corrugated capillaries [148,149].

4. Conclusions

By studying the dynamic historical development in the laser technology arena one cannot avoid noticing a gradual paradigm shift occurring after the introduction of the double-heterojunction laser diodes 40 years ago. Versatility afforded by the structure design, relatively easily exploitable advantages of semiconductor bandgap engineering as well as amenability to mass production gradually formed a thinking which can be summarized as follows: “if the job can be done using laser diodes – use laser diodes”. It might be too bold to claim at this moment in time that a similar paradigm shift will happen in the field of nonlinear optical materials, however the huge progress since the introduction of the electric field poling in 1983 as a means for structuring nonlinearity keep us hopeful that this just might happen in the future. Before it happens, though, a great deal of dedicated effort must be applied in further improvement of suitable nonlinear materials and structuring techniques.

Acknowledgements

The authors acknowledge support from Swedish Research Council (VR) and Alice and Knut Wallenberg foundation.

References

- [1] T.H. Maiman, *Nature* 187 (1960) 493–494.
- [2] L.F. Johnson, K. Nassau, *Proc. IRE* 49 (1961) 1704–1706.
- [3] E. Snitzer, *Phys. Rev. Lett.* 7 (1961) 444–446.
- [4] J.E. Geusic, H.M. Marcos, L.G. Van Uitert, *Appl. Phys. Lett.* 4 (1964) 182–184.
- [5] R.N. Hall, G.E. Fenner, J.D. Kingsley, T.J. Soltyz, R.O. Carlson, *Phys. Rev. Lett.* 9 (1962) 366–368.
- [6] P.A. Franken, A.E. Hill, C.W. Peters, G. Weinreich, *Phys. Rev. Lett.* 7 (1961) 118–119.
- [7] J.A. Giordmaine, *Phys. Rev. Lett.* 8 (1962) 19–20.
- [8] P.D. Maker, R.W. Terhune, M. Nicenoff, C.M. Savage, *Phys. Rev. Lett.* 8 (1962) 21–22.
- [9] J.A. Armstrong, N. Bloembergen, J. Ducuing, P.S. Pershan, *Phys. Rev.* 127 (1962) 1918–1939.
- [10] G.D. Boyd, D.A. Kleinman, *Phys. Rev.* 39 (1968) 3597–3639.
- [11] V.G. Dimitriev, G.G. Gurzadyan, D.N. Nikogosyan, *Handbook of Nonlinear Optical Crystals*, Springer, 1999.
- [12] A. Smith, *Crystal Bibliography*. < <http://www.as-photonics.com/SNLO.html> >.
- [13] C. Chen, B. Wu, A. Jiang, G. You, *Sci. Sin.*, Ser. B 28 (1985) 235–243.
- [14] C. Chen, Y. Wu, A. Jiang, B. Wu, R. Li, Sh. Li, *J. Opt. Soc. Am. B* 6 (1989) 616–621.
- [15] Y. Mori, I. Kuroda, S. Nakajima, T. Sasaki, S. Nakai, *Appl. Phys. Lett.* 67 (1995) 1818–1820.
- [16] P. Becker, J. Liebertz, L. Bohaty, *J. Cryst. Growth* 203 (1999) 149–155.
- [17] B.T. Matthias, J.P. Remeika, *Phys. Rev.* 76 (1949) 1886–1887.
- [18] R.C. Miller, *Appl. Phys. Lett.* 5 (1964) 17–19.
- [19] K. Nassau, H.J. Levinstein, G.M. Loiacono, *J. Chem. Phys. Solids* 27 (1966) 989–996.
- [20] Y. Furukawa, K. Kitamura, S. Takekawa, A. Miyamoto, M. Terao, N. Suda, *Appl. Phys. Lett.* 77 (2000) 2494–2496.
- [21] F.C. Zumsteg, J.D. Bierlein, T.E. Gier, *J. Appl. Phys.* 47 (1976) 4980–4985.
- [22] B. Ray, A.J. Payne, G.J. Burrell, *Phys. Status Solidi* 35 (1969) 197.
- [23] G.D. Boyd, E. Burhler, F.G. Storz, *Appl. Phys. Lett.* 18 (1971) 30–304.
- [24] P.G. Schunemann, K.T. Zawilski, Th.M. Pollak, D.E. Zelmon, N.C. Fernelius, F.K. Hopkins, *ASSP* 2008, January 28, Nara, Japan, Post-Deadline Paper MG6.
- [25] H. Nakanishi, H. Matsuda, S. Okada, M. Kato, *Japan Patent Application No. Toku-Gan-Sho* 61-192404, 1986.
- [26] G. Knöpfle, R. Schlessler, R. Ducret, P. Günter, *Nonlinear Opt.* 9 (1995) 143.
- [27] T. Sasaki, A. Yokotani, *J. Cryst. Growth* 99 (1990) 820–826.
- [28] M. Rothschild, *Optics Photon. News (OSA)* (2010) 27–31.
- [29] J.J. Jacob, A.J. Merriam, *Proc. SPIE* 5567 (1) (2004) 1099–1106.
- [30] J. Merriam, D.S. Bethune, J.A. Hoffnagle, W.D. Hinsberg, C.M. Jefferson, J.J. Jacob, T. Litvin, *Proc. SPIE* 6520 (2007) 65202Z.
- [31] Sh. Sohma, H. Takahashi, T. Taniuchi, H. Ito, *Chem. Phys.* 245 (1999) 359–364.
- [32] G.D. Boyd, C.K.N. Patel, *Appl. Phys. Lett.* 8 (1966) 313–315.
- [33] H. Komine, W.H. Long Jr., J.W. Tully, E.A. Stappaerts, *Opt. Lett.* 23 (1998) 661–663.
- [34] R. Haidar, *Appl. Phys. Lett.* 88 (2006) 211102.
- [35] H. Kogelnik, H.P. Weber, *J. Opt. Soc. Am.* 64 (1974) 174–185.
- [36] M.M. Fejer, G.A. Magel, D.H. Jundt, R.L. Byer, *IEEE J. Quantum Electron.* 28 (1992) 2631–2654.
- [37] M.V. Pack, D.J. Armstrong, A. Smith, *Appl. Opt.* 43 (2004) 3319–3323.
- [38] M.E. Klein, D.-H. Lee, J.-P. Meyn, B. Beier, K.-J. Boller, R. Wallenstein, *Opt. Lett.* 23 (1998) 831–833.
- [39] U. Strossner, A. Peters, J. Mlynek, S. Schiller, J.-P. Meyn, R. Wallenstein, *Opt. Lett.* 24 (1999) 1602–1604.
- [40] G.K. Samanta, G.R. Fayaz, Z. Sun, M. Ebrahim-Zadeh, *Opt. Lett.* 32 (2007) 400–402.
- [41] G.K. Samanta, G.R. Fayaz, M. Ebrahim-Zadeh, *Opt. Lett.* 32 (2007) 2623–2625.
- [42] M. Baudrier-Raybaut, R. Haidar, Ph. Kupecek, Ph. Lemasson, E. Rosencher, *Nature* 432 (2004) 374–376.
- [43] E.Yu. Morozov, A.S. Chiurkin, *Quantum Electron.* 34 (2004) 227–232.
- [44] L.E. Myers, R.C. Eckardt, M.M. Fejer, R.L. Byer, *Optics Lett.* 21 (1996) 591–593.
- [45] P.E. Powers, Th.J. Kulp, S.E. Bison, *Optics Lett.* 23 (1998) 159–161.
- [46] V. Smilgevičius, A. Piskarskas, V. Pasiskevicius, J. Hellström, S. Wang, F. Laurell, *Optics Commun.* 173 (2000) 365.
- [47] J.P. Fève, B. Boulanger, B. Ménaert, O. Picaud, *Optics Lett.* 28 (2003) 1028–1030.
- [48] M.A. Arbore, O. Marco, M.M. Fejer, *Opt. Lett.* 22 (1997) 865–867.
- [49] M. Schober, G. Imeshev, M.M. Fejer, *Opt. Lett.* 27 (2002) 1129–1131.
- [50] K.A. Tillman, D.T. Reid, D. Artigas, J. Hellström, V. Pasiskevicius, F. Laurell, *J. Opt. Soc. Am. B* 20 (2003) 1309.
- [51] M. Charbonneau-Lefort, B. Afeyan, M.M. Fejer, *J. Opt. Soc. Am. B* 27 (2010) 824–841.
- [52] M. Charbonneau-Lefort, M.M. Fejer, B. Afeyan, *Opt. Lett.* 30 (2005) 634–636.
- [53] S.M. Russell, P.E. Powers, M.J. Missey, K.J. Schepler, *IEEE J. Quantum Electron.* 37 (2001) 877–887.
- [54] A. Fragemann, V. Pasiskevicius, F. Laurell, *Opt. Lett.* 30 (2005) 2296–2298.
- [55] S.M. Saltiel, Y.S. Kivshar, *Opt. Lett.* 31 (2006) 3321–3323.
- [56] Sh. Zhu, Y. Zhu, N. Ming, *Science* 278 (1997) 843–846.
- [57] M.H. Chou, K.R. Parameswaran, M.M. Fejer, I. Brener, *Opt. Lett.* 24 (1999) 1157–1159.
- [58] M. Asobe, O. Tadanaga, H. Miyazawa, Y. Nishida, H. Suzuki, *Opt. Lett.* 28 (2003) 558–560.
- [59] A. Bahabad, N. Voloch, A. Arie, R. Lifshitz, *J. Opt. Soc. Am.* 24 (2007) 1916–1921.
- [60] R. Lifshitz, A. Arie, A. Bahabad, *Phys. Rev. Lett.* 95 (2005) 133901.
- [61] G.I. Stegeman, M. Sheik-Bahae, E.W. Van Stryland, G. Asanto, *Opt. Lett.* 18 (1993) 13–15.
- [62] O. Bang, C.B. Clausen, P.L. Christiansen, L. Torner, *Opt. Lett.* 24 (1999) 1413–1415.
- [63] L. Torner, C.B. Clausen, M.M. Fejer, *Opt. Lett.* 23 (1998) 903–905.
- [64] B. Bourliaguet, V. Couderc, A. Barthélémy, G.W. Ross, P.G.R. Smith, D.C. Hanna, C. De Angelis, *Opt. Lett.* 24 (1999) 1410–1412.
- [65] S.J. Holmgren, V. Pasiskevicius, F. Laurell, *Opt. Express* 13 (2005) 5270–5278.
- [66] S.J. Holmgren, V. Pasiskevicius, F. Laurell, *Opt. Express* 14 (2006) 6675.
- [67] B. Jacobsson, V. Pasiskevicius, F. Laurell, V. Smirnov, L. Glebov, *Opt. Lett.* 34 (2009) 449–451.
- [68] P. Martelli, P. Boffi, M. Ferrario, L. Marazzi, P. Parolari, R. Siano, V. Pusino, P. Minzoni, I. Cristiani, C. Langrock, M.M. Fejer, M. Martinelli, V. Degiorgio, *Opt. Express* 17 (2009) 17758–17763.
- [69] A. Tomita, T. Umeke, O. Tadanaga, H. Song, M. Asobe, *Opt. Lett.* 35 (2010) 805–807.
- [70] C. Canalas, V. Pasiskevicius, R. Clemens, F. Laurell, *Appl. Phys. Lett.* 82 (2003) 4233–4235.

- [71] X. Gu, R.Y. Korotkov, Y.J. Ding, J.U. Kang, J.B. Khurgin, J. Opt. Soc. Am. B 15 (1998) 1561–1566.
- [72] X. Mu, I.B. Zotova, Y.J. Ding, J.B. Khurgin, W.P. Risk, Optics Commun. 181 (2000) 153–159.
- [73] C. Canalias, V. Pasiskevicius, M. Fokine, F. Laurell, Appl. Phys. Lett. 86 (2005) 181105.
- [74] S.E. Harris, Appl. Phys. Lett. 9 (1966) 114–116.
- [75] C. Canalias, V. Pasiskevicius, Nature Photon. 1 (2007) 459–462.
- [76] V. Pasiskevicius, C. Canalias, G. Strömqvist, F. Laurell, in: SPIE Proc., vol. 6875, 2008, p. 687508.
- [77] V. Berger, Phys. Rev. Lett. 81 (1998) 4136–4139.
- [78] A. Arie, N. Habsboosh, A. Bahabad, Opt. Quantum Electron. 39 (2007) 361–375.
- [79] N.G.R. Broderick, G.W. Ross, H.L. Offerhaus, D.J. Richardson, D.C. Hanna, Phys. Rev. Lett. 84 (2000) 4345–4348.
- [80] C. Canalias, M. Nordlöf, V. Pasiskevicius, F. Laurell, Appl. Phys. Lett. 94 (2009) 081121.
- [81] T. Ellenbogen, N. Voloch-Bloch, A. Ganany-Padoviz, A. Arie, Nature Photon. 3 (2009) 395–398.
- [82] S. Saltiel, W. Krolikowsky, D. Neshev, Y. Kivshar, Opt. Express 15 (2007) 4132–4138.
- [83] M.S. Pitch, C.D. Cantrell, R.C. Sze, J. Appl. Phys. 47 (1976) 3514–3517.
- [84] A. Szilagyi, A. Hordvik, H. Schlossberg, J. Appl. Phys. 47 (1976) 2025–2032.
- [85] D.E. Thompson, J.d. McMullen, D.B. Andersson, Appl. Phys. Lett. 29 (1976) 113–115.
- [86] M. Okada, K. Takizawa, S. Ieri, Opt. Commun. 18 (1976) 331–334.
- [87] H. Mao, F. Fu, B. Wu, Ch. Chen, Appl. Phys. Lett. 61 (1992) 1148–1150.
- [88] Y. Okuno, K. Uomi, M. Aoki, T. Tsuchiya, IEEE J. Quantum Electron. 33 (1997) 959–969.
- [89] E. Lallier, M. Brevignon, J. Lehoux, Opt. Lett. 23 (1998) 1511–1513.
- [90] T. Mitsui, J. Furuichi, Phys. Rev. 90 (1953) 193–202.
- [91] R. Matthias, A. von Hippel, Phys. Rev. 73 (1948) 1387.
- [92] R.C. Miller, A. Savage, Phys. Rev. Lett. 2 (1959) 294–296.
- [93] D. Feng, N.-B. Ming, J.-F. Hong, Y.-Sh. Yang, J.-S. Zhu, Zh. Yang, Y.-N. Wang, Appl. Phys. Lett. 37 (1980) 607–609.
- [94] W.S. Wang, Q. Zhou, Z.H. Geng, D. Feng, J. Cryst. Growth 79 (1986) 706–709.
- [95] K. Nakamura, H. Shimizu, in: IEEE Ultrasonics Symp., 1983, pp. 527–530.
- [96] J. Webjörn, F. Laurell, G. Arvidsson, IEEE J. Lightwave Technol. 7 (1989) 1597.
- [97] E.J. Lim, M.M. Fejer, R.L. Byer, W.J. Kozlovsky, Electron. Lett. 25 (1989) 731.
- [98] C.J. van der Poel, J.D. Bierlein, J.B. Brown, Appl. Phys. Lett. 57 (1990) 2074–2076.
- [99] M. Yamada, N. Nada, M. Saitoh, K. Watanabe, Appl. Phys. Lett. 62 (1993) 435–437.
- [100] K.R. Parameswaran, J.R. Kurtz, R.V. Rousev, M.M. Fejer, Opt. Lett. 27 (2002) 43–45.
- [101] O. Tadanaga, T. Yanagawa, Y. Nishida, H. Miyazawa, K. Magari, M. Asobe, H. Suzuki, Appl. Phys. Lett. 88 (2006) 061101.
- [102] W.P. Risk, S.D. Lau, Appl. Phys. Lett. 69 (1996) 3999–4001.
- [103] A. Jechow, S. McNeil, C. Kaleva, D. Skoczowsky, R. Menzel, in: Proc. SPIE, vol. 7197, 2009, p. 719707.
- [104] M.B. Oron, S. Pearl, P. Blau, S. Shusterman, Opt. Lett. 35 (2010) 2678–2680.
- [105] X. Yu, L. Scaccabarozzi, J.S. Harris, P.S. Kuo, M.M. Fejer, Opt. Express 13 (2005) 10742–10748.
- [106] J. Webjörn, V. Pruneri, P. St. J. Russel, J.R.M. Barr, D.C. Hanna, Electron. Lett. 30 (1994) 894.
- [107] L.E. Myers, R.C. Eckardt, M.M. Fejer, R.L. Byer, W.R. Bosenberg, J.W. Pierce, J. Opt. Soc. Am. B 12 (1995) 2102–2116.
- [108] G.D. Miller, R.G. Batchko, M.M. Fejer, R.L. Byer, in: Proc. SPIE, vol. 2700, 1996, pp. 34–45.
- [109] R.G. Batchko, V.Y. Shur, M.M. Fejer, R.L. Boyd, Appl. Phys. Lett. 75 (1999) 1673–1675.
- [110] Q. Chen, W.P. Risk, Electron. Lett. 30 (1994) 1516–1517.
- [111] H. Karlsson, F. Laurell, Appl. Phys. Lett. 71 (1997) 3474–3476.
- [112] G. Rosenman, A. Skliar, D. Eger, M. Oron, M. Katz, Appl. Phys. Lett. 73 (1998) 3650–3652.
- [113] H. Karlsson, F. Laurell, P. Henriksson, G. Arvidsson, Electron. Lett. 32 (1996) 556–557.
- [114] A. Fragemann, V. Pasiskevicius, J. Nordborg, J. Hellström, F. Laurell, Appl. Phys. Lett. 83 (2003) 3090–3092.
- [115] A. Zukauskas, N. Thilmann, C. Canalias, V. Pasiskevicius, F. Laurell, Appl. Phys. Lett. 95 (2009) 191103.
- [116] Wang, V. Pasiskevicius, H. Karlsson, F. Laurell, Opt. Lett. 23 (1998) 1883–1885.
- [117] M. Peltz, U. Bäder, A. Borzutzky, R. Wallenstein, J. Hellström, H. Karlsson, V. Pasiskevicius, F. Laurell, Appl. Phys. B 73 (2001) 663–670.
- [118] R.G. Batchko, G.D. Miller, A. Alexandrovski, M.M. Fejer, R.L. Byer, 1998 OSA Technical Digest Series Optical Society of America, Washington, DC, vol. 12, 1998, pp. 75–76.
- [119] S. Wang, V. Pasiskevicius, F. Laurell, J. Appl. Phys. 95 (2004) 2023–2028.
- [120] G. Zhong, J. Jian, Z. Wu, in: Proceedings of the 11th International Quantum Electronics Conference, IEEE Cat. No. 80, CH 1561-0, 1980, p. 631.
- [121] A. Kuroda, S. Kurimura, Y. Uesu, Appl. Phys. Lett. 69 (1996) 1565–1567.
- [122] H. Ishizuki, T. Taira, Opt. Lett. 30 (2005) 2918–2920.
- [123] Y. Furukawa, K. Kitamura, A. Alexandrovski, R.K. Route, M.M. Fejer, G. Foulon, Appl. Phys. Lett. 78 (2001) 1970–1972.
- [124] Y. Furukawa, K. Kitamura, E. Suzuki, K. Niwa, J. Cryst. Growth 197 (1999) 889–895.
- [125] M. Katz, R.K. Route, D.S. Hum, K.R. Parameswaran, G.D. Miller, M.M. Fejer, Opt. Lett. 29 (2004) 1775–1777.
- [126] J. Hirohashi, V. Pasiskevicius, S. Wang, F. Laurell, J. Appl. Phys. 101 (2007) 033105.
- [127] H. Ishizuki, T. Taira, Opt. Express 18 (2010) 253–258.
- [128] P.A. Thomas, R. Duhlev, S.J. Teat, Acta Cryst. B 50 (1994) 538–543.
- [129] R. Kriegel, R. Wellendorf, Ch. Kaps, Mater. Res. Bull. 36 (2001) 245–252.
- [130] Q. Jiang, P.A. Thomas, K.B. Hutton, R.C.C. Ward, J. Appl. Phys. 92 (2002) 2717–2723.
- [131] S. Wang, V. Pasiskevicius, F. Laurell, Opt. Mater. 30 (2007) 594–599.
- [132] A. Zukauskas, V. Pasiskevicius, F. Laurell, C. Canalias CLEO/QELS:2010, Technical Digest, CMG3, 2010.
- [133] A. Zukauskas, N. Thilmann, V. Pasiskevicius, F. Laurell, C. Canalias, Opt. Mater. Express 1 (2011) 201–206.
- [134] A. Peña, B. Ménaert, B. Boulanger, F. Laurell, C. Canalias, V. Pasiskevicius, P. Segonds, J. Debray, S. Pairis, Opt. Mater. Express 1 (2011) 185–191.
- [135] L.A. Eyres, P.J. Tourreau, T.J. Pinguet, C.B. Ebert, J.S. Harris, M.M. Fejer, L. Becouarn, B. Gérard, E. Lallier, Appl. Phys. Lett. 79 (2001) 904–906.
- [136] D. Faye, E. Lallier, A. Grisard, B. Gérard, in: Proc. SPIE, vol. 6740, 2007, p. 674001.
- [137] S.D. Setzler, P.G. Shunemann, T.M. Pollak, L.A. Pomeranz, M.J. Missey, D.E. Zelmon, OSA TOPS v. 26 Advanced Solid State Lasers 676–680, 1999.
- [138] M. Horowitz, A. Bekker, B. Fischer, Appl. Phys. Lett. 62 (1993) 2619–2621.
- [139] Y.Y. Zhu, J.S. Fu, R.F. Xiao, G.K.L. Wong, Appl. Phys. Lett. 70 (1997) 1793–1795.
- [140] J.-P. Meyn, M.E. Klein, D. Woll, R. Wallenstein, D. Rytz, Opt. Lett. 24 (1999) 1154.
- [141] J. Hirohashi, K. Yamada, H. Kamio, S. Shichijyo, Jpn. J. Appl. Phys. 43 (2004) 559.
- [142] J. Hirohashi, V. Pasiskevicius, Appl. Phys. B 81 (2005) 761–763.
- [143] R.A. Myers, N. Mukherjee, s.R.J. Brueck, Opt. Lett. 16 (1991) 1732–1734.
- [144] S.C. Buchter, T.Y. Fan, V. Liberman, J.J. Zayhowsky, M. Rothschild, E.J. Mason, A. Cassanho, H.P. Janssen, J.H. Burnett, Opt. Lett. 26 (2001) 1693–1695.
- [145] M. Harada, K. Muramatsu, Y. Iwasaki, S. Kurimura, T. Taira, J. Mater. Res. 19 (2004) 969–972.
- [146] A. Chowdhury, H.M. Ng, M. Bhardwaj, N.G. Weimann, Appl. Phys. Lett. 83 (2003) 1077–1079.
- [147] S. Kitamura, M. Adachi, J. Nakanishi, K. Hayashi, OSA Topical meeting Advanced Solid State Photonics, Technical Digest, TuB2, 2008.
- [148] A. Paul, R.A. Bartels, R. Tobey, H. Green, S. Weiman, I.P. Christov, M.M. Murnane, H.C. Kapteyn, S. Backus, Nature 421 (2003) 51–54.
- [149] A. Bahabad, M.M. Murnane, H.C. Kapteyn, Nature Photon. 4 (2010) 570–575.